Excitation of an electronic band structure by a single-photon Fock state

H. Rose[1], A. N. Vasil'ev[2,3], O. V. Tikhonova[2,3], T. Meier[1], and P. R. Sharapova[1]

[1]Paderborn University, Department of Physics, Warburger Straße 100, D-33098 Paderborn, Germany
[2]Faculty of Physics, Lomonosov Moscow State University, Moscow, Russia
[3]Skobeltsyn Institute of Nuclear Physics, Lomonosov Moscow State University, Moscow, Russia

1 Introduction

Semiconductor nanonstructures have received significant attention over the last decades as their optical and electronic properties can differ drastically from bulk materials, due to the reduction in size down to just a few nanometers. One classifies semiconductor nanostructures by the number of dimensions in which carriers can move freely, leading to quantum dots (quasi 0D materials), quantum wires (quasi 1D materials), and quantum wells (quasi 2D materials) [1, 2]. Their remarkable and designable optical properties gave rise to many research areas and are still investigated intensively [3–5]. One of the rather novel fields is semiconductor quantum optics, in which the light-matter interaction is described on a fully-quantized level by the coupling to photon states [6]. Since quantum light includes more degrees of freedom and information than classical light [7, 8], several aspects in this field are not yet well understood.

In this report, we consider a semiconductor nanostructure in an optical cavity that is coupled to quantum light. We describe the semiconductor nanostructure with a parabolic band structure in a 1D k-space, while we assume a single-mode quantum field. The 1D system is chosen for simplicity in both the analytical and the numerical treatment and paves the way for the description of 2D structures in the future. Therefore, instead of using parameters which are realistic for 1D systems, we rather use parameters which qualitatively correspond to 2D GaAs structures.

2 Theoretical Model

The electronic band structure in k-space is modeled by an arrangement of two-level systems (TLS) whose transition energy corresponds the difference between conduction and

valence band energy at the respective k-point. The interaction between the band structure and the single-mode quantum light field is described by a Jaynes-Cummings type Hamiltonian for the respective TLS, where the rotating wave approximation (RWA) is applied. This leads to the following Hamiltonian:

$$\hat{H} = \sum_{\boldsymbol{k}} \left[\epsilon^v_{\boldsymbol{k}} a^\dagger_{v,\boldsymbol{k}} a_{v,\boldsymbol{k}} + \epsilon^c_{\boldsymbol{k}} a^\dagger_{c,\boldsymbol{k}} a_{c,\boldsymbol{k}} \right] + \hbar\nu \left[B^\dagger B + \frac{1}{2} \right] - \sum_{\boldsymbol{k}} M_{\boldsymbol{k}} (B^\dagger a^\dagger_{v,\boldsymbol{k}} a_{c,\boldsymbol{k}} + B a^\dagger_{c,\boldsymbol{k}} a_{v,\boldsymbol{k}}), \quad (1)$$

where $\epsilon^\lambda_{\boldsymbol{k}}$ is the band energy, $a^\dagger_{\lambda,\boldsymbol{k}}$ ($a_{\lambda,\boldsymbol{k}}$) are the creation (annihilation) operators of an electron in the respective band $\lambda = c, v$, while $B^\dagger$ (B) is the creation (annihilation) operator of a photon, and $M_{\boldsymbol{k}}$ is the light-matter coupling.

When treating N points in k-space (N k-points), it is convenient to introduce the following notation to denote the respective excitation level:

$$\lambda_1, \lambda_2, ..., \lambda_j, ..., \lambda_N = (\lambda), \quad (2)$$
$$\lambda_1, \lambda_2, ..., \lambda_j + 1, ..., \lambda_N = (\lambda|\lambda_j + 1), \quad (3)$$
$$\lambda_1, \lambda_2, ..., \lambda_j - 1, ..., \lambda_N = (\lambda|\lambda_j - 1), \quad (4)$$
$$\lambda_1, \lambda_2, ..., \lambda_{j-1}, \tilde{\lambda}, \lambda_{j+1}, ..., \lambda_N = (\lambda|\lambda_j = \tilde{\lambda}), \quad (5)$$
$$v, v, ..., v, v = (v), \quad (6)$$

where λ_i can either be v for valence band or c for conduction band and denotes whether the electron at the i-th k-point is in the valence or conduction band. Adding or subtracting a 1 can be understood as promoting or demoting an electron, i.e., $v + 1 = c$ and $c - 1 = v$.

The state vector of the system can be written as

$$|\Psi\rangle = \sum_{(\lambda)}^{v,c} \sum_{n=0}^{\infty} c^{(\lambda)}_n e^{\frac{1}{i\hbar} E^{(\lambda)}_n t} \, |(\lambda), n\rangle \,, \quad (7)$$

where $c^{(\lambda)}_n$ are the probability amplitudes and $E^{(\lambda)}_n$ are the energies for the respective basis states $|(\lambda), n\rangle$, n denotes the n-Fock state. Substituting Eq. (7) into the Schrödinger equation yields equations of motion for the probability amplitudes:

$$\begin{aligned} -i\hbar\partial_t c^{(\lambda)}_n = &\sum_{i=1}^{N} M_{\boldsymbol{k}_i} c^{(\lambda|\lambda_i+1)}_{n-1} e^{-i\Delta_{\boldsymbol{k}_i} t} \sqrt{n} \delta_{\lambda_i, v}, \\ &+ \sum_{i=1}^{N} M_{\boldsymbol{k}_i} c^{(\lambda|\lambda_i-1)}_{n+1} e^{i\Delta_{\boldsymbol{k}_i} t} \sqrt{n+1} \delta_{\lambda_i, c}, \end{aligned} \quad (8)$$

where $\Delta_{\boldsymbol{k}} = \omega_{\boldsymbol{k}} - \nu$ is the detuning between the band structure of the material $\omega_{\boldsymbol{k}}$ and the optical frequency of the quantum field ν.

This energy difference determines the type and dimension of the described semiconductor. We restrict our investigation to 1D materials, such as quantum wires, and proceed with a parabolic dispersion, which is a good approximation in the vicinity of the band gap for direct semiconductors:

$$\hbar\omega_k = \hbar\omega_g + \frac{\hbar^2}{2m_r} k^2 = \hbar\omega_g + \alpha\tilde{k}^2, \quad (9)$$

where m_r is the reduced electron-hole mass and k is the momentum. We choose α in such a way that it has the unit of an energy while $\tilde{k}$ is dimensionless. For GaAs-based semiconductor nanostructures the parabolic dispersion is valid for some 10 meV's above the band gap. The reduced electron-hole mass for such systems is $m_r = 0.056 m_0$, where m_0 is the mass of a free electron [9]. The choice of $\alpha = 10$ meV and a maximum value for $\tilde{k}$ of $k_{\max} = 1$ corresponds to a section of around 4-5% of the first Brillouin zone, centered around the Γ-point. In our work, we fix the value for α and increase $k_{\max}$, leading to energetically higher points, which, however, have only a small influence on the dynamics. This is done to assure that the features at small energies are covered.

Figure 1 demonstrates the parabolic band structure inside the interval $[-k_{\max}, k_{\max}]$, leading to a maximum considered energy of $E_{\max} = \alpha k_{\max}^2$.

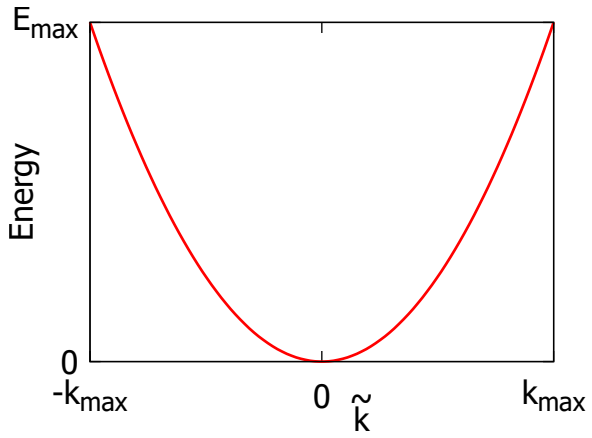

Figure 1: Illustration of the parabolic band structure in the interval $[-k_{\max}, k_{\max}]$.

The first sum on the right-hand side of Eq. (8) describes the demotion of an electron from the conduction to the valence band under the emission of a photon, while the second sum describes the promotion of an electron from the valence to the conduction band under the absorption of a photon.

There are several observables that can be studied within this model, obtained by computing expectation values of the respective operators. In this way, the conduction/valence band occupation for the point k_i can be computed from

$$O_c^{k_i} = \sum_{n=0}^{\infty} \sum_{\lambda \neq \lambda_i} |c_n^{(\lambda|\lambda_i = c)}|^2, \tag{10}$$

$$O_v^{k_i} = \sum_{n=0}^{\infty} \sum_{\lambda \neq \lambda_i} |c_n^{(\lambda|\lambda_i = v)}|^2 = 1 - O_c^{k_i}. \tag{11}$$

The ground-state probability is given by:

$$O_{\text{ground}} = \sum_{n=0}^{\infty} |c_n^{(v)}|^2, \tag{12}$$

which corresponds to the case where no electronic excitation is present.

2.1 Single Photon

For the case that the quantum field is given by a single-photon Fock state at the initial moment of time, Eq. (8) can be simplified into the following form:

$$\partial_t c_1^{(v)} = \frac{i}{\hbar} \sum_{l=1}^{N} M_{\boldsymbol{k}_l} c_0^{(v|\lambda_l=c)} e^{-i\Delta_{\boldsymbol{k}_l} t}, \tag{13}$$

$$\partial_t c_0^{(v|\lambda_j=c)} = \frac{i}{\hbar} M_{\boldsymbol{k}_j} c_1^{(v)} e^{i\Delta_{\boldsymbol{k}_j} t}, \tag{14}$$

where $c_1^{(v)}$ is the probability amplitude for all TLS being in the ground state while the single photon is present, whereas $c_0^{(v|\lambda_j=c)}$ is the probability amplitude for the state in which the field is in the vacuum state while the TLS at k_j is excited. Eqs. (10)-(12) for the observables are simplified as follows:

$$O_c^{k_i} = |c_0^{(\lambda|\lambda_i=c)}|^2, \tag{15}$$

$$O_{\text{ground}} = |c_1^{(v)}|^2. \tag{16}$$

Note that our system, which includes a single photon and a two-band semiconductor, describes kind of the inverse situation as a system made of a two-level atom and a photonic band gap which has been discussed in [10]. Since on the level considered here, interchanging the electron and photon operators is possible, Eqs. (13) and (14) are formally equivalent to those presented in [10], however describe the reverse physical situation.

2.2 Convergence

When describing the continuous k-space with a finite number of discrete points one needs to make sure to consider a sufficient number of points, so that the continuum is modeled correctly. However, a different number of k-points corresponds to a different system. The decisive quantity that needs to be conserved while changing the number of k-points is the total oscillator strength Ω, which is given by

$$\Omega = \sum_{i=1}^{N} |M_{\boldsymbol{k}_i}|^2. \tag{17}$$

Henceforth, we consider a light-matter coupling that does not depend on k. In this case, one can directly conclude that in order to conserve the total oscillator strength of the system, the coupling parameter should be rescaled with the number of k-points N as follows:

$$M = \frac{M^0}{\sqrt{N}} \Rightarrow \Omega = |M^0|^2, \tag{18}$$

where M^0 is a constant and we assume the same coupling parameter for each TLS. Furthermore, it should be noted that the total oscillator strength corresponds to a fixed interval in k-space, which means that increasing this interval will increase the oscillator

strength Ω. This becomes relevant when a close vicinity around the Γ-point is considered, since changing the size of this region will also change the oscillator strength. Taking this fact into account, we will use the following expression for M:

$$M = \sqrt{k_{\max}} \frac{M^0}{\sqrt{N}}. \tag{19}$$

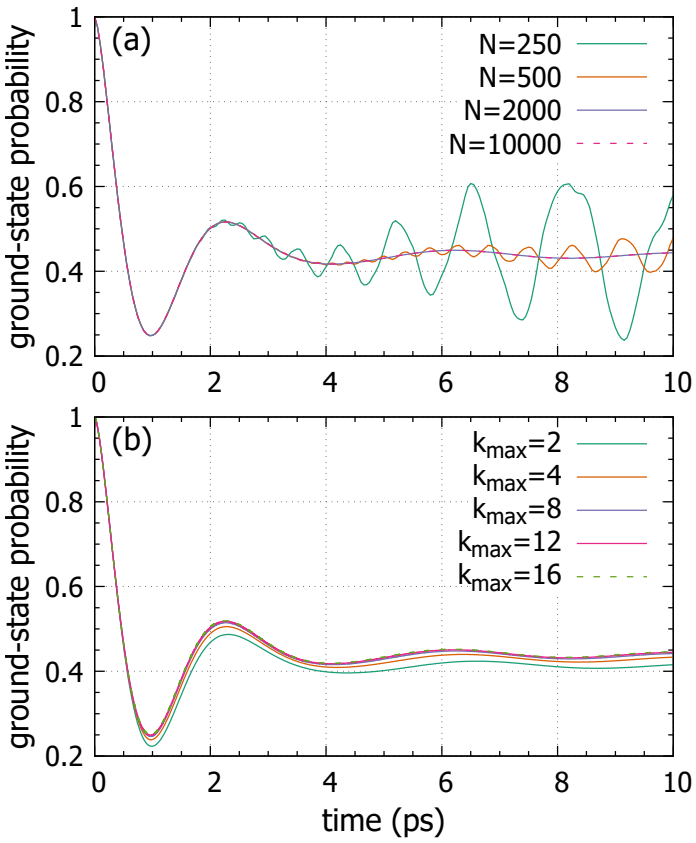

Figure 2: Ground-state probability for a single photon and a parabolic band structure with $\alpha = 10$ meV. Here and in all further calculations, only the valence band is populated at the initial moment of time. (a) $k_{\max} = 10$ and a different amount of k-points N is considered. (b) $N = 10^4$ and different k-intervals $[-k_{\max}, k_{\max}]$ are taken into account.

Figure 2 shows the dynamics of the ground-state probability O_{ground} for different amounts of k-points N and different k-intervals $[-k_{\max}, k_{\max}]$. Simulations are performed for a parabolic dispersion with $\alpha = 10$ meV and $M^0 = 1.5$ meV, which is a reasonable choice for GaAs quantum wells confined in a microcavity [11]. In Fig. 2(a) a k-interval with $k_{\max} = 10$ is considered, which leads to the maximum energy of $E_{max} = 1$ eV. One can observe that for a small amount of k-points (e.g. $N = 250$ or $N = 500$) oscillations that disrupt the correct dynamics are present. The correct dynamics can be simulated with a sufficiently large amount of k-points. The required number of k-points depends on the maximum energy that is considered in the band structure and on the simulation time. Fig. 2(b) demonstrates the convergence of the ground-state probability dynamics

O_{ground} with increasing the interval $[-k_{\max}, k_{\max}]$ in k-space, here, the number of k-points is chosen as $N = 10000$. One can see that all simulations show a similar dynamics, while the probability slightly increases for increasing the considered energy range. This strengthens the suitability of our model, since the relevant contributions are contained in a small energy range. We proceed with $k_{\max} = 10$ for all subsequent simulations to cover all dynamics in the investigated range, while the most important ones are enclosed in around $k_{\max} = 1.5$, as can be seen later in Section 4.

3 Analytical approach

We apply a Fourier transform to the linear system Eqs. (13), (14). The secular equation for determining the quasi-energies of this system can be written in the form

$$\hbar\Delta - \gamma = \sum_{j=-L}^{L} \frac{M_j^2}{\alpha(k_{\max} j/L\,)^2 - \gamma} = G\,(\gamma)\,, \tag{20}$$

where γ is the shift of the quasi-energy $\hbar\omega_g + \gamma$ from the band gap $\hbar\omega_g$ and $N = 2L+1$ is the total number of k-points. Here, Δ is the corresponding shift of the photon frequency $\nu = \omega_g + \Delta$ from the band gap frequency ω_g, $M_j = \sqrt{k_{\max}} M^0/\sqrt{2L}$.

Introducing dimensionless variables

$$x = \frac{\gamma L^2}{\alpha k_{\max}^2}, \quad \delta = \frac{\hbar\Delta L^2}{\alpha k_{\max}^2}, \quad \beta = \frac{(M^0)^2 L^3}{2\alpha^2 k_{\max}^3}, \tag{21}$$

Eq. (20) can be rewritten in the following form:

$$\delta - x = \sum_{j=-L}^{L} \frac{\beta}{j^2 - x}. \tag{22}$$

The sum in Eq. (22) converges, therefore, for $L >> 1$ we can neglect the sums $\sum_{j=L+1}^{\infty} \frac{1}{j^2-x}$ and $\sum_{j=-\infty}^{-L-1} \frac{1}{j^2-x}$, and thus can expand the limits to infinity. Then the sum in Eq. (22) can be calculated as follows:

$$\sum_{j=-\infty}^{\infty} \frac{1}{j^2 - x} = \begin{cases} -\pi \cot\left(\pi\sqrt{x}\right)/\sqrt{x}, & x > 0 \\ \pi \coth\left(\pi\sqrt{|x|}\right)/\sqrt{|x|}, & x < 0. \end{cases} \tag{23}$$

Substituting Eq. (23) in Eq. (22), one can find that the last equation has one negative root x_0 and L positive roots x_i (taking into account the degeneracy of states with the same $|j|$). The equation for negative $x < 0$ and $\beta >> 1$ is reduced to $\delta + |x| = \beta\pi/\sqrt{|x|}$. For δ=0, the negative eigenvalue equals to $x_0 = -(\beta\pi)^{2/3}$, positive eigenvalues are given by

$$x_i \approx \left((i-1) + \frac{1}{\pi} \text{arccot}\left(\frac{(i-1)^3}{\beta\pi} \right) \right)^2, \tag{24}$$

where $i = 1, 2, \cdots L$. These quasi-energies are shown in the top-left panel of Fig. 3.

If at the initial moment of time the field is represented by a single photon, while only the valence band is populated, the ground-state probability amplitude is given by

$$c_1^{(v)}(t) = \exp(i\omega_g t) \sum_{m=0}^{L} \frac{\exp(i\gamma_m t/\hbar)}{1 + \sum\limits_{j=-L}^{L} \frac{M^2}{\left(\alpha(k_{\max} j/L)^2 - \gamma_m\right)^2}} = \exp(i\omega_g t) \sum_{m=0}^{L} \frac{\exp(i\gamma_m t/\hbar)}{1 + \frac{dG(\gamma)}{d\gamma}\Big|_{\gamma=\gamma_m}}. \quad (25)$$

.

The weight of the negative eigenvalue can be evaluated as

$$\left(1 + \frac{dG(\gamma)}{d\gamma}\right)^{-1}\Bigg|_{\gamma=\gamma_0} = \left(1 + \beta\frac{\pi}{2|x|^{3/2}}\right)^{-1}\Bigg|_{x=-(\beta\pi)^{2/3}} = \frac{2}{3}, \quad (26)$$

while the weights of positive eigenvalues x_i can be calculated as follows

$$\left(1 + \frac{dG(\gamma)}{d\gamma}\right)^{-1}\Bigg|_{\gamma=\gamma_i} = \left(1 + \beta\frac{\pi\cot(\pi\sqrt{x})}{2x^{3/2}} + \beta\frac{\pi^2\left(1 + \cot(\pi\sqrt{x})^2\right)}{2x}\right)^{-1}\Bigg|_{x=x_i}$$

$$= \left(\frac{3}{2} + \beta\frac{\pi^2}{2x}\left(1 + \frac{x^3}{\pi^2\beta^2}\right)\right)^{-1}\Bigg|_{x=x_i}. \quad (27)$$

In the case of $\beta >> 1$, the last equation simplifies to:

$$\left(1 + \frac{dG(\gamma)}{d\gamma}\right)^{-1}\Bigg|_{\gamma=\gamma_i} \approx \frac{2y}{\pi(\pi\beta)^{1/3}(1+y^3)}\Bigg|_{y=(i-1)^2/(\pi\beta)^{2/3}}. \quad (28)$$

This function has a maximum at $y \approx 1$ which corresponds to $x_i \approx -x_0 = (\beta\pi)^{2/3}$. For a single photon at the initial moment of time, the weights of the "dressed" eigenstates corresponding to these quasi-energies are shown in the two top panels of Fig. 3.

Combining Eqs. (26- 28) with Eq. (25), the ground-state probability amplitude takes a form

$$c_1^{(v)}(t)\, e^{-i\omega_g t} = \frac{2}{3}\exp(-i\mu|x_0|\, t)$$

$$+ \sum_{m=1}^{L} \frac{2(m-1)^2/|x_0|}{\pi\sqrt{|x_0|}\left(1 + \left((m-1)^2/|x_0|\right)^3\right)} \exp\left(i\mu(m-1)^2 t\right) \quad (29)$$

$$\approx \frac{2}{3}\exp(-i\mu|x_0|\, t) + \int_0^{\infty} \frac{2z^2/|x_0|}{\pi\sqrt{|x_0|}\left(1 + (z^2/|x_0|)^3\right)} \exp\left(i\,\mu z^2 t\right) dz \quad (30)$$

$$= \frac{1}{3}\left(\exp(-i\mu|x_0|\, t) + 2\exp\left(\frac{1}{2}i\mu|x_0|\, t\right)\cosh\left(\frac{\sqrt{3}}{2}\mu|x_0|\, t\right)\right.$$

$$\left. - 2(1+i)\sqrt{\frac{2}{\pi}}(\mu|x_0|\, t)^{3/2}\, {}_1F_3\left(1; \frac{5}{6}, \frac{7}{6}, \frac{3}{2}; \frac{1}{27}i(\mu|x_0|\, t)^3\right)\right). \quad (31)$$

Here $\mu = \alpha k_{\max}^2/\hbar L^2$ and ${}_1F_3(a_1; b_1, b_2, b_3; z)$ is a hypergeometric function. Fig. 4 shows the ground-state probability calculated using the expression given above. The asymptotic value of the probability at large times is $(2/3)^2 = 4/9 \approx 0.4444$ (the integral in the Eq. (30) vanishes due to the interference of distributed positive frequencies). The bottom panel in Fig. 3 shows the evolution of the electron-hole states with time.

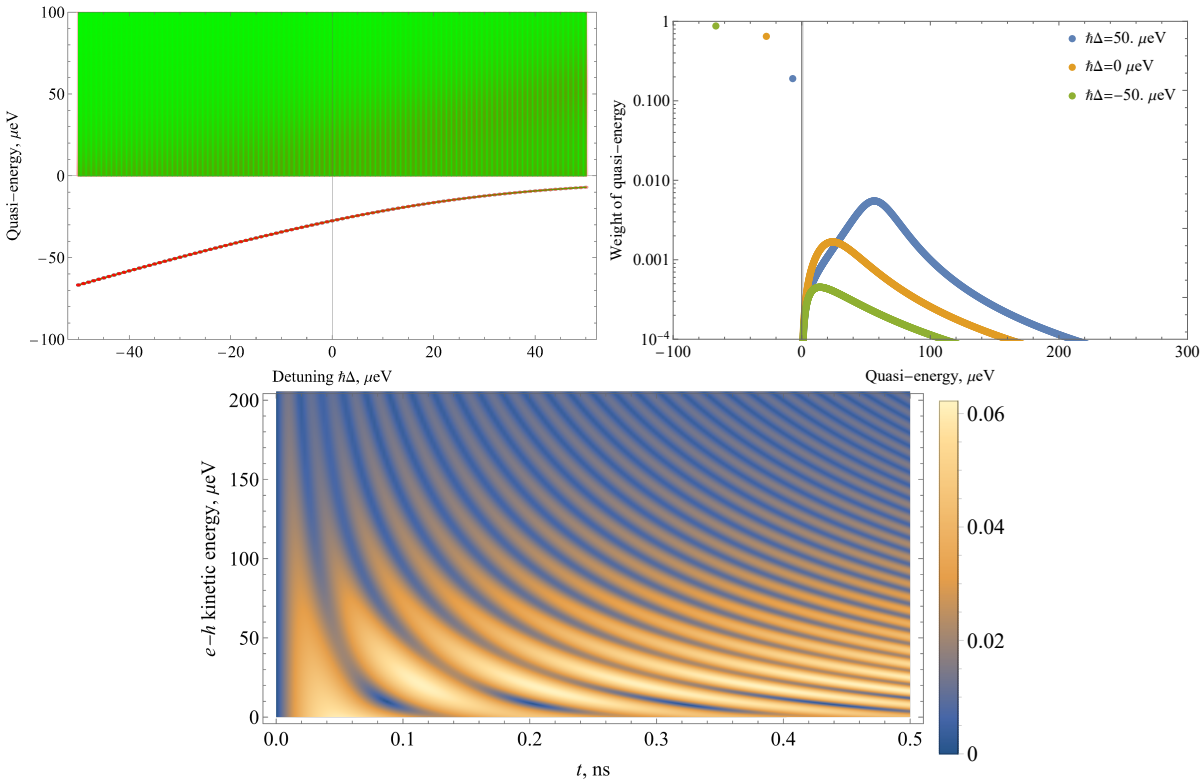

Figure 3: Distribution of quasi-energies in the case of a single photon at the initial moment of time, while only the valence band is populated. Top left panel: Green lines present positive quasi-energies γ versus detuning Δ. Red dots correspond to the negative quasi-energy γ_0. The intensities of the red and green colors indicate the weights of the respective "dressed" states, which is more clearly illustrated in the top-right figure. Top right: Weights of "dressed" states for three values of detunings Δ. Bottom panel: Evolution of the square root of the conduction-band occupation for different energies in the case of $\Delta = 0$. The calculations were performed for N=80000, α=10 meV, k_{max}=10, M^0=0.1 meV.

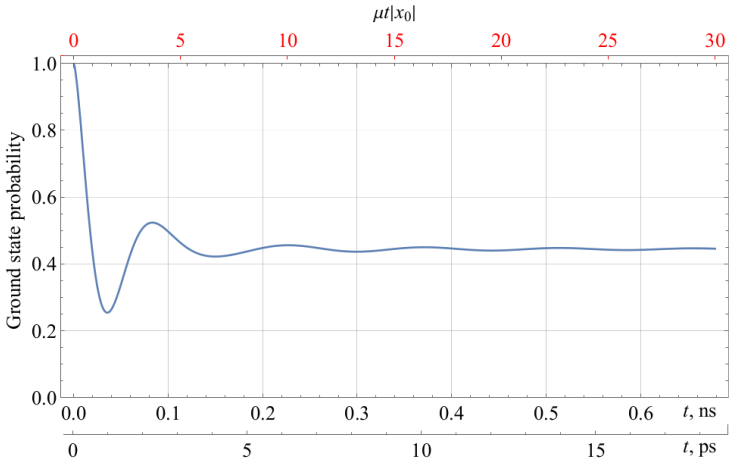

Figure 4: Ground-state probability $\left|c_1^{(v)}(t)\right|^2$ calculated using the analytical result, i.e., Eq. (31). The axis above the plot refers to dimensionless time, the upper scale below the plot refers to times calculated for parameters used in Fig. 3, the lower scale below the plot refers to times calculated for parameters used in numerical calculations in Fig. 5.

4 Numerical results

In correspondence with the analytical treatment, we do our numerical investigation considering a single photon. While the ground-state probability already yields a characteristic property of the system, it may not reflect its full complexity. Therefore, it is advantageous to consider the dynamics at individual k-points. Figure 5(a) shows the time evolution of the conduction-band occupation $O_c^{k_i}$ for different k-points, while Fig. 5(b) shows the corresponding ground-state probability. Note that only smaller section of the computed interval with $k_{\max} = 10$ is presented, since it contains all relevant features. One can see that the conduction-band occupation oscillates in time, with the frequency $\Delta_{\boldsymbol{k_i}}$. We can obtain a relation between the ground-state probability and the conduction-band occupation from the normalization condition:

$$O_{\text{ground}} + \sum_i O_c^{\boldsymbol{k}_i} = |c_1^{(v)}|^2 + \sum_i |c_0^{(\lambda|\lambda_i=c)}|^2 = 1. \tag{32}$$

Thus, we can conclude that the summation of oscillations with different frequencies will eventually lead to destructive interference, and therefore results in a cancellation of the time dynamics of the ground-state probability, as seen in Fig. 5.

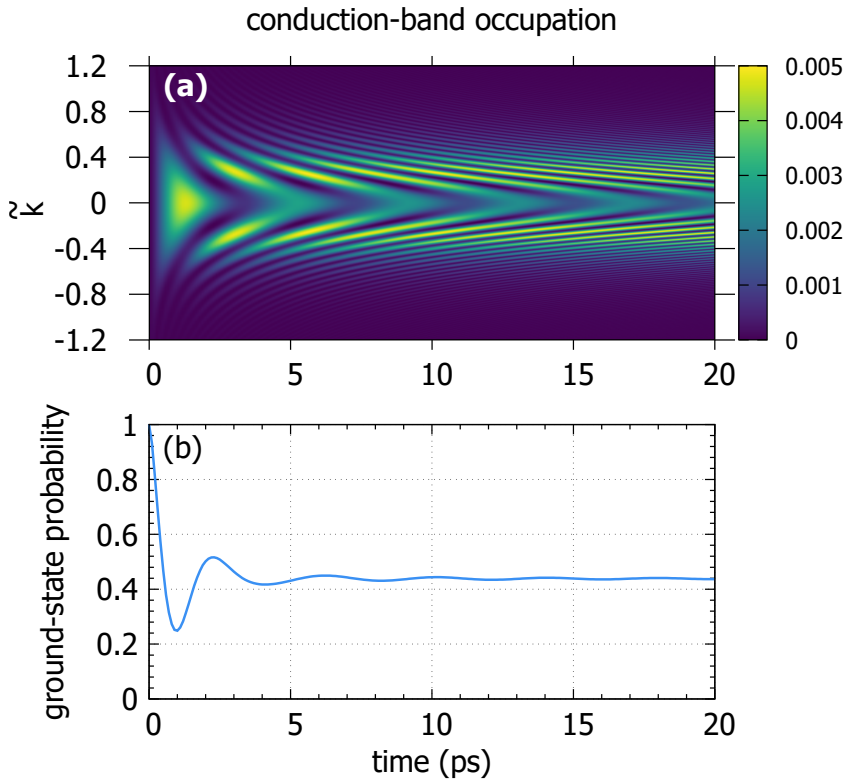

Figure 5: (a) Conduction-band occupations for different k-point indices over time (b) ground-state probability. (Parameters: $\alpha = 10\text{meV}$, $N = 5001$, $k_{\max} = 10$)

Next, we consider our system being excited with different optical frequencies, i.e., the electronic system is not excited resonantly at the band gap, but we introduce an energetic offset $\hbar\Delta$, so that $\nu = \omega_g + \Delta$. This means, $\Delta < 0$ describes an excitation below the band-gap energy, while $\Delta > 0$ leads to a situation in which the excitation is above the band-gap energy, allowing to resonantly excite electrons at higher transition energies.

Figure 6 shows O_{ground} for the energetic offsets $\hbar\Delta = -2$ meV, -1 meV, 0 meV, 1 meV, and 2 meV. One can observe that negative offsets lead to a higher ground-state probability, and a faster dynamics with more oscillations, while the opposite case is found for positive offsets. Qualitatively, this behavior is clear, since in the case of negative offsets, the detuning $\Delta_{\boldsymbol{k}_i}$ is positive for all k-points, which means that none of the k-points is excited resonantly, resulting in a less efficient excitation. By contrast, positive offsets allow for resonant excitations within the band. This behavior can be further analyzed by considering the conduction-band occupation.

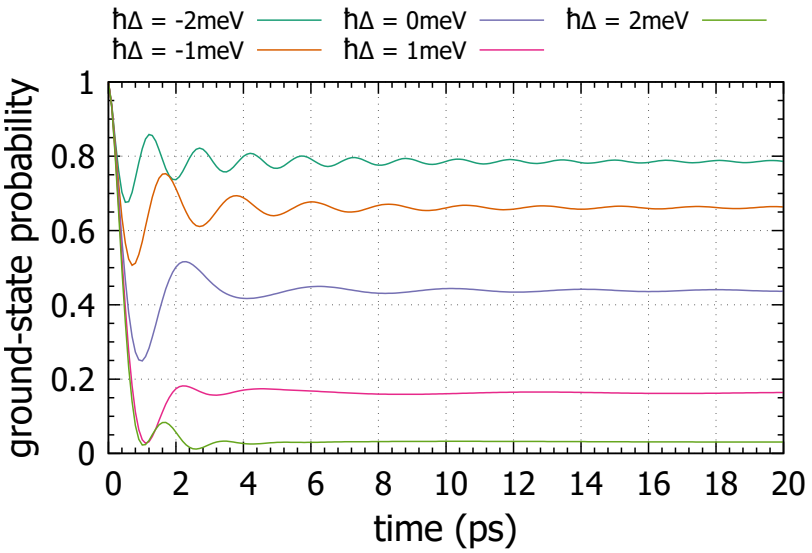

Figure 6: Ground-state probability for different optical frequencies ν of the quantum field, measured as a detuning with respect to the band gap frequency ω_g, i.e. $\Delta = \nu - \omega_g$. (Parameters: $\alpha = 10\text{meV}$, $N = 5001$, $k_{\max} = 10$)

Figure 7 shows the conduction-band occupation for different energetic offsets. A negative offset leads to a larger positive detuning $\Delta_{\boldsymbol{k}_i}$ for the respective k-points, resulting in faster oscillations with a smaller magnitude in time. This is consistent with the ground-state probability from Fig. 6, which exhibits faster oscillations at a higher value. In contrast, positive offsets lead to the formation of two stripes, which for large enough offsets appear at the resonantly excited k-points, i.e. where $\Delta_{\boldsymbol{k}_i} = 0$. As can be seen in the top-left graph in Fig. 3, the eigenvalue that is energetically below the band gap (red curve) tends to zero with the increase in the energetic offset $\hbar\Delta$. As it is follows from the analytical treatment, this eigenvalue is responsible for the long-time dynamics of the ground-state probability. Therefore, with increasing the energetic offset, the excitation of this dressed state is less efficient, resulting in a lower probability of populating the ground state at large times. At the same time, for quasi-energies that are above the band gap, the peak in the weights is formed with an increase in the energetic offset, as can be seen in the top-right graph in Fig. 3. The appearance of such a maximum in positive quasi-energies leads to the formation of the stripes in the conduction-band occupation, as shown in Fig.7. Thus, the decrease of the ground-state probability and the appearance of two stripes in the conduction-band occupation with increasing energetic offsets are caused by new eigenstates that are formed during the light-matter interaction. We note that this discussion is related to the discussion in Ref. [10], however, in this case for an inverse system to ours.

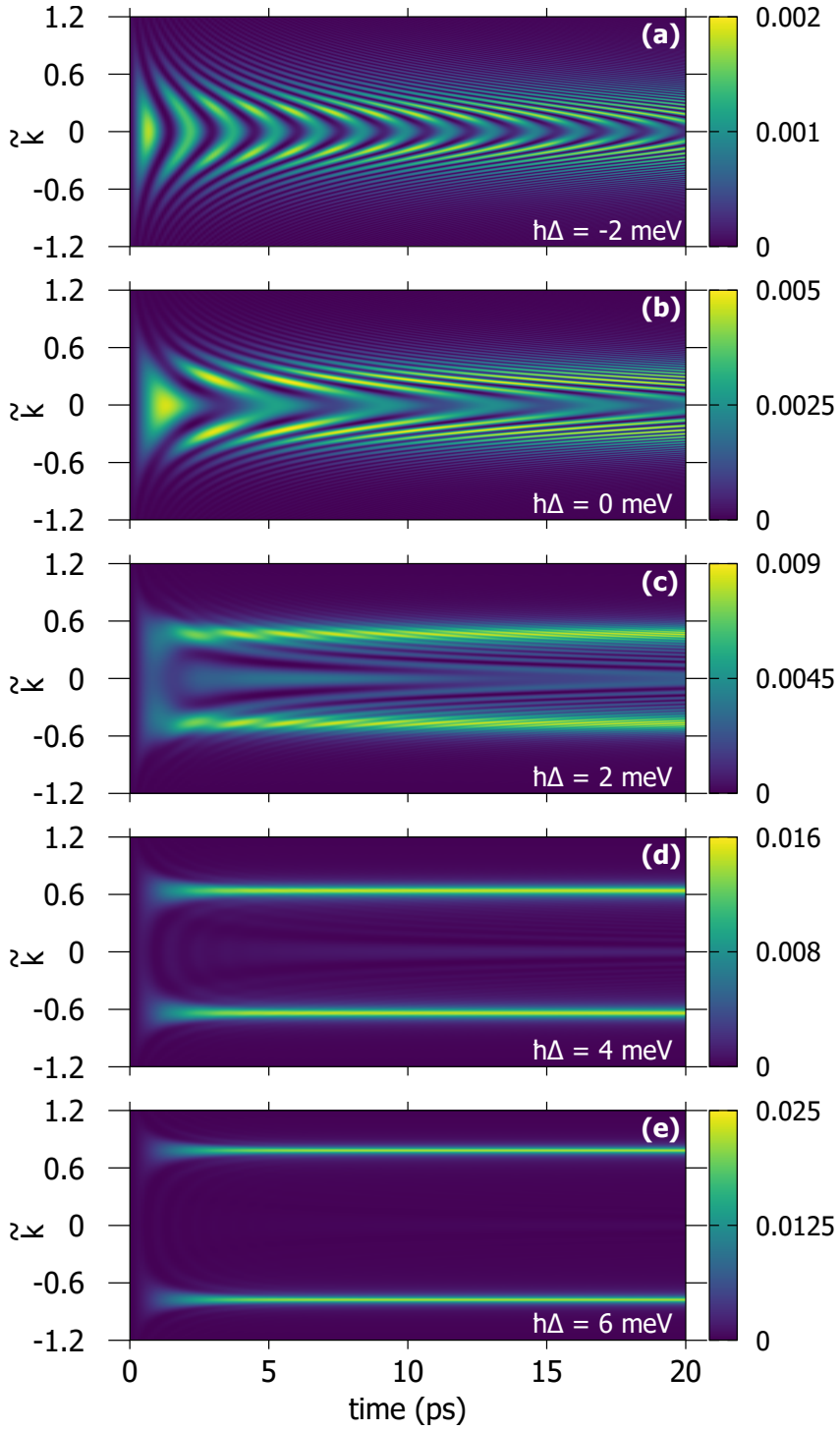

Figure 7: The dynamics of the conduction-band occupation is shown for $\alpha = 10$ meV, $N = 5001$, and $k_{\max} = 10$. The energetic offset $\hbar\Delta$ is chosen as (a) -2 meV, (b) 0 meV, (c) 2 meV, (d) 4 meV, and (e) 6 meV.

5 Conclusion

We present a model which describes the quantum-optical dynamics of an electronic band structure which is excited by a single-photon Fock state both analytically and numerically. We obtain an approximate analytical solution for the ground-state probability, i.e., the probability that all electronic states remain unexcited. Remarkably, this solution depends only on a single eigenstate with the energy below the band gap. For a resonant excitation with respect to the band gap, we find a steady-state probability equals to 4/9, which does not depend on other parameters. This is accounted to the dressed state that corresponds to the aforementioned quasi-energy, which has no decay during the dynamics. Complementing, we perform numerical simulations which allow a deeper insight into the dynamics. Here, we demonstrate that the dynamics of the ground-state probability and the formation of stripes in the conduction-band probability strongly depend on the detuning from the band gap and gained physical understanding by considering the corresponding conduction-band occupation.

The results shown in this report demonstrate consequences of a microscopic description of semiconductor nanostructures that exhibit a quantum-optical excitation and pave the way to further investigations of more complex scenarios. These include the consideration of multi-photon light states, or systems of different dimensions, where especially the two-dimensional case is of interest, that allows the description of semiconductor quantum wells.

Acknowledgments

Support by the joint grant of the Deutsche Forschungsgemeinschaft (DFG) and the Russian Science Foundation (RSF) (projects SH 1228/2-1, ME 1916/7-1, No.19-42-04105) is gratefully acknowledged.

References

[1] C. W. J. Beenakker and H. van Houten, Quantum Transport in Semiconductor Nanostructures, Solid State Physics **44**, 1 (1991).

[2] D. Bimberg, *Semiconductor Nanostructures* (Springer, Berlin, 2008).

[3] H. Haug and S. W. Koch, *Quantum Theory of the Optical and Electronic Properties of Semiconductors*, 4th ed. (World Scientific, Singapore, 2005).

[4] J. Shah, *Ultrafast Spectroscopy of Semiconductors and Semiconductor Nanostructures* (Springer, Berlin, 1996).

[5] T. Meier, P. Thomas, and S. W. Koch, *Coherent Semiconductor Optics: From Basic Concepts to Nanostructure Applications* (Springer, New York, 2007).

[6] M. Kira and S. W. Koch, *Semiconductor Quantum Optics* (Cambridge University Press, Cambridge, 2012).

[7] S. Mukamel et al., Roadmap on quantum light spectroscopy, J. Phys. B: At., Mol., Opt. Phys. **53**, 072002 (2020).

[8] M. O. Scully and M. S. Zubairy, *Quantum Optics* (Cambridge Univ. Press, Cambridge, 1997).

[9] M. Levinshtein, S. Rumyantsev, and M. Shur, *Handbook Series on Semiconductor Parameters* (World Scientific, Singapore, 1999), Vol. 2.

[10] S. John and T. Quang, Spontaneous emission near the edge of a photonic band gap, Phys. Rev. A **50**, 1764 (1994).

[11] H. Rose, J. Paul, J. K. Wahlstrand, A. D. Bristow, and T. Meier, Theoretical analysis and simulations of two-dimensional Fourier transform spectroscopy performed on excitonpolaritons of a quantum-well microcavity system, Proc. SPIE **11684**, 1168414 (2021).